

Organometallic Chemistry

Electron density distribution in vanadocene ($\eta^5\text{-C}_5\text{H}_5\text{)}_2\text{V}$ and mixed metallocenes ($\eta^5\text{-C}_5\text{H}_5\text{)}\text{M}(\eta^5\text{-C}_7\text{H}_7)$ ($\text{M} = \text{Ti, V, or Cr}$) and ($\eta^5\text{-C}_5\text{H}_5\text{)}\text{Ti}(\eta^8\text{-C}_8\text{H}_8)$. Effect of the nature of the cyclic ligand on the character of the $\text{M}-(\pi\text{-ligand})$ bond

K. A. Lyssenko,^{a*} M. Yu. Antipin,^a and S. Yu. Ketkov^b

^aA. N. Nesmeyanov Institute of Organoelement Compounds, Russian Academy of Sciences,
28 ul. Vavilova, 117813 Moscow, Russian Federation.

Fax: +7 (095) 135 5085. E-mail: kostya@xrlab.ineos.ac.ru

^bG. A. Razuvayev Institute of Organometallic Compounds, Russian Academy of Sciences,
49 ul. Tropinina, 603600 Nizhni Novgorod, Russian Federation.

Fax: +7 (831) 266 1497. E-mail: sketkov@imoc.sinn.ru

The electron density distribution and atomic displacements were analyzed based on the results of precision low-temperature X-ray diffraction studies of a series of isostructural ($Pnma$, $Z = 4$) mixed metallocenes ($\eta^5\text{-C}_5\text{H}_5\text{)}\text{M}(\eta^5\text{-C}_7\text{H}_7)$ ($\text{M} = \text{Ti, V, or Cr}$) and ($\eta^5\text{-C}_5\text{H}_5\text{)}\text{Ti}(\eta^8\text{-C}_8\text{H}_8)$. The barriers to rotation of the cyclic ligands were evaluated based on rms libration amplitudes. Analysis of the deformation electron density demonstrated that the character of the $\text{M}-(\pi\text{-ligand})$ chemical bond depends substantially both on the nature of the metal atom and the size of the ligand. Lowering of the local symmetry of the ($\eta^5\text{-C}_5\text{H}_5\text{)}\text{M}(\eta^5\text{-C}_7\text{H}_7$) complexes to C_5 leads to distortion of the cylindrical symmetry of the electron density distribution observed in vanadocene ($\eta^5\text{-C}_5\text{H}_5\text{)}_2\text{V}$ and titanocene ($\eta^5\text{-C}_5\text{H}_5\text{)}\text{Ti}(\eta^8\text{-C}_8\text{H}_8)$.

Key words: metallocenes, cycloheptatrienyl and cyclooctatetraenyl ligands, electron density distribution, chemical bond.

The discovery of ferrocene ($\eta^5\text{-C}_5\text{H}_5\text{)}_2\text{Fe}$ in 1951 and the unambiguous determination of its structure gave impetus to the rise and development of the modern

structural chemistry of organometallic compounds.^{1,2} Cyclopentadienyl (Cp) complexes of most of the transition metals and of a number of main-group metals^{1–3}

and mixed sandwich complexes with cyclic ligands of the $\text{CpM}(\eta^n\text{-C}_n\text{H}_n)$ type (where $n = 3-8$)³⁻⁵ and their heteroanalogs¹ have been prepared and structurally characterized.

Since the first theoretical study by the molecular orbital (MO) method,⁶ the fundamental qualitative concepts of the electronic structures of metallocenes have remained virtually unchanged.⁵ When analyzing the structures of symmetrical and mixed metallocenes, it is generally assumed that the d orbitals of the metal atom in the pseudoaxial ligand field are transformed into bonding e_2 ($d_{x^2-y^2}$, d_{xy}), nonbonding a_1 (d_{z^2}), and antibonding e_1 (d_{xz} , d_{yz}) molecular orbitals. Studies of symmetrical complexes of the Cp_2M type, *viz.*, $(\eta^6\text{-C}_6\text{H}_6)_2\text{M}^{7,8}$ and mixed complexes containing the cycloheptatrienyl (Ch, C_7H_7) and cyclooctatetraenyl (Cot, C_8H_8) ligands,⁹⁻¹¹ by ultraviolet photoelectron spectroscopy and quantum-chemical methods (INDO)⁴ demonstrated that the molecular orbital a_1 is predominantly atomic in character irrespective of the type of the cyclic ligand. To the contrary, e_1 and e_2 MOs make the major contribution to the formation of the metal-ligand bond. In the case of the Cp ligand, the e_1 orbitals of the metal atom and the corresponding e_1 orbitals of Cp are mixed. The electron transfer from the metal atom to the ligand through the e_2 ($\text{M} \rightarrow e_2$ (ligand)) interaction becomes dominant as the size of the ligand increases due to a decrease in the energy of the e_2 and e_1 orbitals of the ligand in the series of C_6H_6 (Bz), C_7H_7 , and C_8H_8 . Thus, quantum-chemical calculations of the complexes with the Cot ligands by the INDO method¹³ demonstrated that the lowest e_2 MO of the ligand is virtually not mixed with the orbitals of the metal atom corresponding in symmetry, which results in the change in the usual order of the MO arrangement ($e_2 < a_1 < e_1$). In this case, the a_1 orbital becomes the lowest one, whereas e_2 MO, unlike those in symmetrical (Cp_2M) and mixed (CpMCh and CpMBz) metallocenes, becomes antibonding. For example, calculations by the INDO method showed that the Ti atom in the CpTiCot complex has the a_1^1 configuration and the contribution of the Cot ligand to e_2 MO is larger than 80%.¹³ To the contrary, the metal atom in the isoelectronic CpVCh complex has the $e_2^4a_1^1$ configuration and the contribution of the ligand to e_2 MO is smaller than 60%.¹⁴

The above-mentioned estimates of the degrees of mixing of the orbitals of the metal atom and the ligand are inconsistent with the formal description of the charge distribution in the complexes within the framework of the Hückel rule ($4n + 2$). According to this rule, the Ch ligand is aromatic both if the charge is +1 and -3, whereas the Cot ligand is aromatic only if the charge is -2. Therefore, the oxidation state of the metal atom in mixed CpMCh complexes can be taken to be equal to zero and +4 in the case of the positively and negatively charged Ch ligand, respectively. Analogously, the formal charge +3 should be assigned to the metal atom in the CpMCot complexes.

Needless to say, the oxidation state of the metal atom serves as the formal approximation for the description of the charge distribution in metallocenes, which is actually determined both by donation of electrons from the metal atom to the ligand and by back π -donation.¹ If the contribution of the metal atom to the e_2 orbital is taken to be approximately 50%, the charges of the Ch ligand and the metal atom are -1 and +2, respectively. Analogously, the charge of the Cot ligand is equal to zero rather than to -2 as follows from the Hückel rule.

It was long believed that the Ch ligand bears the charge +1.^{5,15-17} This charge was qualitatively evaluated by chemical studies of the methylation products of CpMCh complexes¹⁸ and by physicochemical methods, *viz.*, by X-ray photoelectron spectroscopy (XPS)^{18,19,21} and ultraviolet photoelectron spectroscopy.^{9-11,16,20}

However, analysis of the published data demonstrated that the charges -3 and +1, which were formally assigned to the Ch ligand, and the charge -2 assigned to the Cot ligand are inconsistent with the actual character of the chemical bonds in metallocenes CpMCh and CpMCot . Moreover, detailed studies by photoelectron spectroscopy with the use of a helium source^{9,10} and synchrotron radiation¹¹ revealed that the chemical bonds in these compounds and particularly the contribution of the d orbitals to MOs of metallocenes depend substantially on the nature of the metal atom.

With the aim of revealing the effect of the nature of metal and the size of the cyclic ligand on the character of the $\text{M}-(\pi\text{-ligand})$ interaction by experimental methods, we studied the electron density distribution $\rho(r)$ based on the X-ray diffraction data for a series of symmetrical and mixed metallocenes, *viz.*, for 15-electron vanadocene Cp_2V (**1**), 16-electron CpTiCh (**2**), 17-electron CpVCh (**3**) and CpTiCot (**5**), and 18-electron CpCrCh (**4**).

Results and Discussion

X-ray diffraction study of "mixed" metallocenes. Earlier, the crystal structures of metallocenes have been studied by X-ray diffraction analysis with different experimental accuracy. However, investigations of the electron density distribution based on the X-ray diffraction data have not been performed, except for qualitative analysis of phosphaferrocene $(\eta^5\text{-C}_5\text{H}_5)\text{Fe}[\eta^5\text{-PC}_4\text{H}_2(\text{CH}_3)_2]$,²² the triple-decker sandwich complex $(\eta^5\text{-C}_5\text{H}_5)\text{V}(\eta^6\text{-C}_6\text{H}_6)\text{V}(\eta^5\text{-C}_5\text{H}_5)$,²³ and vanadocene $(\eta^5\text{-C}_5\text{H}_5)_2\text{V}$.²⁴ The electron density distribution in some compounds containing the cyclopentadienyl and benzene ligands, in particular, in $(\eta^6\text{-C}_6\text{H}_6)\text{Cr}(\text{CO})_3$,²⁵ $[(\eta^5\text{-C}_5\text{H}_5)\text{Fe}(\text{CO})_2]_2$,²⁶ and $[(\eta^5\text{-C}_5\text{H}_5)\text{Ni}_2(\mu\text{-C}_2\text{H}_2)]$, were examined.²⁷ Experimental studies of the electron density distribution in organometallic compounds containing the Ch and Cot ligands are not documented either. Investigations of $\rho(r)$ in different organometallic compounds were surveyed in the reviews.²⁸⁻³⁰

Studies of the electron density distribution in metallocenes are often hampered due to the presence of the disorder in the crystals observed in a wide temperature range and to phase transitions (see Ref. 31 and references therein). Hence, in studies of $\rho(r)$ in the crystals of complexes **1**–**5**, we gave considerable attention to analysis of the parameters of anisotropic atomic displacements and to examination of the possible disorder of the rings.

The principal crystal-structural characteristics of vanadocene in the temperature range of 108–357 K have been studied previously in detail³¹ (Table 1, Figs. 1 and 2). Analysis of the anisotropic atomic displacements in the crystal of Cp_2V demonstrated that the structure is ordered only at 108 K, whereas two positions of the disordered Cp ring can be distinguished in the crystal even at 170 K. The ordered arrangement of the vanadocene molecules at 108 K was confirmed by analy-

sis of the anisotropic atomic displacements within the framework of the LST rigid-body model.³² At this temperature, the bond lengths satisfy Hirshfeld's test for the "bond rigidity,"³³ whereas the largest eigenvalue (L_1) of the libration tensor L is only 31 deg².³¹ For comparison, the L_1 values in the Cp_2V complex at 170 and 297 K are 82 and 91 deg², respectively. It should be emphasized that only the structure of vanadocene in the formally isostructural series of the monoclinic crystals of 3d-metallocenes Cp_2M ($\text{M} = \text{V}, \text{Fe}, \text{Co}, \text{or Ni}$) under study appears to be ordered at low temperature. Until recently, it is this behavior of crystals of simple 3d-metallocenes that restricted experimental investigation of the electron density distribution in these compounds by X-ray diffraction analysis.

Unlike symmetrical 3d-metallocenes studied in detail, mixed complexes have been studied previously only by conventional X-ray diffraction methods at room tempera-

Table 1. Principal crystallographic data and details of refinement of complexes **2**–**5**

Parameter	2	3	4	5
Molecular formula	$\text{C}_{12}\text{H}_{12}\text{Ti}$	$\text{C}_{12}\text{H}_{12}\text{V}$	$\text{C}_{12}\text{H}_{12}\text{Cr}$	$\text{C}_{13}\text{H}_{13}\text{Ti}$
M	204.12	207.16	208.22	217.12
$a/\text{\AA}$	10.921(1)	10.896(1)	10.918(2)	10.992(2)
$b/\text{\AA}$	10.657(1)	10.643(1)	10.704(2)	10.817(3)
$c/\text{\AA}$	7.971(1)	7.883(1)	7.814(1)	8.571(2)
$V/\text{\AA}^3$	927.6(2)	914.2(2)	913.1(2)	1019.1(4)
Z	4	4	4	4
Space group	$Pnma$	$Pnma$	$Pnma$	$Pnma$
$F(000)$	424	428	432	452
μ/cm^1	8.65	10.26	11.94	7.92
$d_{\text{calc}}/\text{g cm}^{-3}$	1.462	1.505	1.515	1.415
T/K	150	150	150	203
$2\theta_{\text{max}}/\text{deg}$	85	86	100	80
Number of measured reflections	15239	7133	14793	8976
$R(\text{int})$	0.0284	0.0470	0.0660	0.0500
Number of independent reflections	3407	3504	4966	2590
R_1 (reflections with $I > 2\sigma(I)$)	0.0306	0.0399	0.0345	0.0446
	(based on 2789 refl.)	(based on 2789 refl.)	(based on 2509 refl.)	(based on 1598 refl.)
wR_2 (all reflections)	0.0975	0.0958	0.0946	0.1026
GOF	0.984	0.968	0.964	1.022
Parameters in the refinement	90	90	90	94

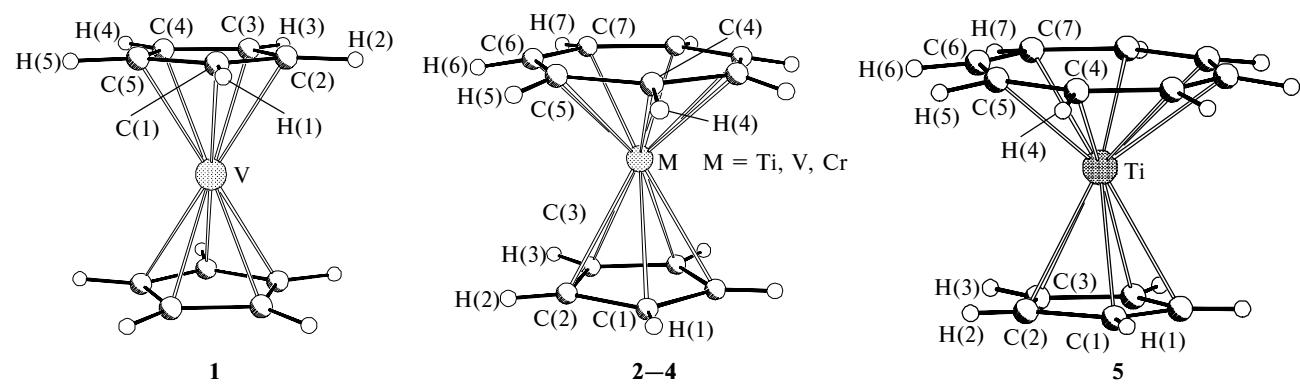


Fig. 1. Overall views of metallocenes **1**–**5**.

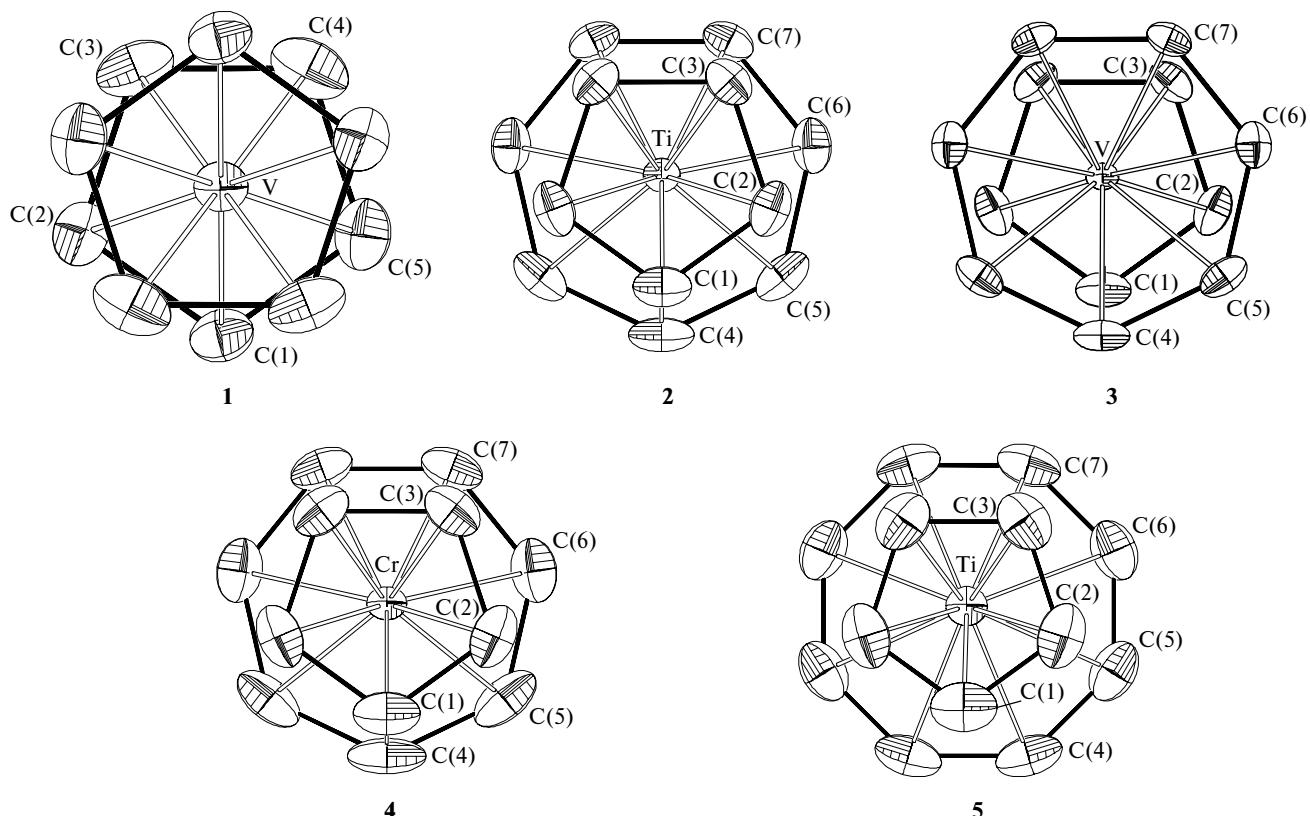


Fig. 2. Projections of metallocenes **1–5** along the metal–center-of-the-ring axis; the atoms are represented as probability ellipsoids ($p = 50\%$) of thermal vibrations.

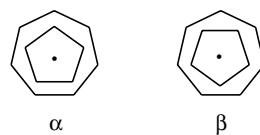
ture (CpTiCh ,³⁴ CpVCh ,³⁵ CpCrCh ,* and CpTiCot ³⁶). In the present work, we studied mixed metallocenes **2**, **3**, and **4** at 150 K and metallocene **5** at 203 K. The latter was studied at higher temperature because the crystals of **5** were destroyed at lower temperature due to the phase transition of the unknown nature.

Compounds **2–5** are isostructural (space group $Pnma$, $Z = 4$, see Table 1). This suggests that the maxima and minima of the deformation electron density observed in the vicinity of the metal atoms of these complexes are associated predominantly with the electronic configurations of the metal atoms and the nature of the ligands.

The principal geometric parameters of complexes **1–5** are given in Tables 2 and 3. The general views of the molecules are shown in Figs. 1 and 2 (the data for vanadocene **1** are given for comparison). In crystals of **2–5**, the molecules are located on crystallographic planes m (symmetry C_s) passing through the H(1), C(1), M (Ti, Cr, or V), C(4), and H(4) atoms (in complexes **2–4** with the Ch ligands) or through the Ti, C(1), and H(1) atoms (in complex **5** with the Cot ligand).

It should be noted that the symmetry C_s of the complexes in the crystals and the limiting molecular symmetry in the series of compounds **2–5** coincide. In

the CpMCh complexes, the symmetry C_s can occur with different mutual arrangements of the Cp and Ch ligands. Analysis of the data available in the Cambridge Structural Database (CSD) demonstrated that unsubstituted metallocenes are characterized by the mutual arrangement of the Cp and Ch ligands such that the atoms lying on the symmetry plane are located one above the other (the *cis* arrangement, the α type). To the contrary, in the methylated complexes ($\eta^5\text{-C}_5\text{Me}_5$)MCh (M = Ti, Zr, or Hf; the reference codes ("refcodes") in CSD are DIXJOJ, GITVAG, and GITVEK, respectively), the atoms lying on the symmetry plane are in *trans* orientations (β type). In the crystal structures of the CpMCh derivatives, the local symmetry C_s is also observed if the molecule occupies a general position. For example, the deviation from the C_s symmetry in the $\text{ChV}[\eta^5\text{-}(\text{C}_5\text{H}_4\text{CO}_2\text{H})]$ (NEWFEA) and $[\eta^5\text{-}(\text{C}_5\text{H}_4\text{SPh})]\text{V}[\eta^7\text{-}(\text{C}_7\text{H}_6\text{SPh})]$ (LEXHAX) complexes with the β -type mutual arrangement of the rings is 0.5° and 3° , respectively.



The principal geometric characteristics of the CpMCh complexes are independent of the mutual arrangement

* The structure of CpCrCh was established by R. D. Russel (cited in Ref. 18)

Table 2. Bond lengths in complexes **1–5**

Com- pound	Method of deter- mination*	Bond length/Å					
		Cp ligand			Ch or Cot ligand		
		C–C	M–C	M–Cp	C–C	M–C	M–Ch (M–Cot)
1	I	1.413(1)–1.423(1)	2.260(1)–2.278(1)	1.922	—	—	—
	II	1.422–1.432 ^a	2.268–2.284				
	III	1.417/1.426 ^b	2.269/2.275				
2	I	1.409(1)–1.414(1)	2.3213(8)–2.3375(8)	1.982	1.416(1)–1.427(1)	2.202(1)/2.2165(6)	1.487
	II	1.417–1.421	2.327–2.343		1.423–1.434	2.210–2.224	
	III	1.412/1.420	2.333/2.336		1.422/1.429	2.212/2.219	
3	I	1.415(1)–1.417(1)	2.252(1)–2.2652(7)	1.917	1.413(1)–1.419(1)	2.183(1)–2.1975(7)	1.464
	II	1.421–1.422	2.251–2.273		1.419–1.425	2.189–2.203	
	III	1.416(1)/1.422	2.261/2.264		1.416/1.422	2.191/2.197	
4	I	1.407(1)–1.411(1)	2.178(1)–2.1954(8)	1.830	1.395(1)–1.411(2)	2.147(1)–2.1669(9)	1.434
	II	1.419–1.423	2.186–2.204		1.418–1.423	2.160–2.179	
	III	1.409/1.421	2.187/2.195		1.402/1.414	2.160/2.172	
5	I	1.400(2)–1.413(2)	2.344(2)–2.363(1)	2.029	1.394(2)–1.406(2)	2.326(2)–2.333(1)	1.441
	II	1.409–1.423	2.353–2.371		1.403–1.415	2.337–2.343	
	III	1.406/1.415	2.353/2.361		1.401/1.410	2.330/2.342	

* I, experiment; II, libration corrections were applied; III, the average value/the average value taking into account the libration corrections. The M–Cp bond corresponds to the distance from the M atom to the center of the ring.

of the rings. Interestingly, complexes of two types (α and β) are present in the structure of $\text{ChV}[\eta^5\text{-(C}_5\text{H}_4\text{CO}_2\text{H)}]$ (the refcode NEWFIE).

In all structures under examination, the Cp and Ch ligands and the Cp and Cot ligands are parallel to one another (the angle between the planes of the cyclic ligands is no higher than 2.6°). However, the deviations of the hydrogen atoms from the mean plane of the ligands are substantially different in character. Previously,³⁷ it has been mentioned that the hydrogen atoms in the coordinated cyclic ligands of the $\eta^n\text{-C}_n\text{H}_n$ type with $n < 5$ are directed away from the metal atom, whereas the hydrogen atoms in larger ligands ($n > 6$) are, on the contrary, inclined to the metal atom. In the case of the Cp ligand, the hydrogen atoms lie almost ideally in the plane of the ring.³⁶ This arrangement is generally attributed to the fact that the p orbitals of the ligand are no longer perpendicular to the plane of the ring to achieve the maximum overlapping with the 3d orbitals of the metal atom resulting in deviations of the hydrogen atoms (Fig. 3).

In all compounds studied in this work, the average angles between the C–H bond and the planes of the Ch

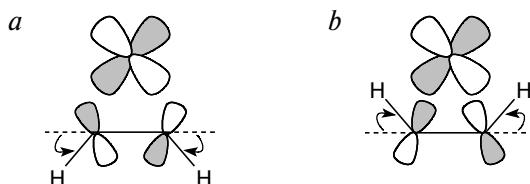


Fig. 3. Deviations of the hydrogen atoms from the plane of the cyclic C_nH_n ligand in the metal π -complexes depending on the size of the ligand: $n < 5$ (a) and $n > 6$ (b).

Table 3. Bond angles in complexes **1–5**

Com- pound	Angle C–C–C/deg	
	Cp ligand	Ch or Cot ligand
1	110.7(1)/108.5; 108.0*	—
2	107.72(4)–108.25(9); 108.4*	128.31(9)–128.72(4); 128.54*
3	107.74(7)–108.3(1); 108.04*	128.35(8)–128.70(4); 128.54*
4	107.77(8)–108.2(1); 108.03*	128.37(9)–128.89(6); 128.54*
5	107.87(9)–108.1(1); 108.0*	134.96(9)–135.04(9); 135.00*

* The average value.

and Cot ligands (9.7° and 9.1° , respectively) are higher than the analogous values in the Cp ligands (on the average, by 1.1°). The exception is the H(1) atom in the Cp ligand in complexes **2–5**, which is located on the crystallographic symmetry plane and for which the corresponding angle in all structures (on the average, 6.3°) is comparable with the analogous values in the Ch and Cot ligands. To the contrary, all angles between the C–H bonds and the plane of the Cp ring in the CpTiCot compound are equal (1.6°). In all complexes under study, the hydrogen atoms deviate from the planes of the cyclic ligands toward the metal atoms.

Analysis of thermal vibrations in the crystals. To reveal the characteristic features of libration vibrations of the rings and the possibility of their disorder in the crystals of the compounds under study, which affect the electron density distribution, we took into account the libration corrections for thermal motion of the molecules in the approximation of the LTS rigid-body model.³² Calculation were carried out with the use of the

THMA-11 program.³⁸ If the libration motion is taken into account, not only the expected elongation of the C—C and M—C bonds is observed, but also the lengths of the chemically equivalent bonds are equalized (Table 2). The agreement between the experimental parameters of anisotropic thermal motion (U_{ij}) and the corresponding values calculated within the framework of the rigid-body model is sufficiently good ($R_u = 5.1\text{--}9.6\%$, $\langle \Delta U^2 \rangle^{1/2} = 0.0012\text{--}0.0020 \text{ \AA}^2$, $\sigma \langle U^2 \rangle^{1/2} = 0.0010 \text{ \AA}^2$). Calculations of the differences between the rms "oncoming" displacements (Δ) demonstrated that the Cp, Ch, and Cot ligands in these complexes are structurally rigid;³³ the average Δ value for all C—C bonds in the rings is no higher than $8 \cdot 10^{-4} \text{ \AA}^2$. At the same time, the rms Δ values for pairs of the carbon atoms, which are not linked through the chemical bond and belong to different ligands, are substantially larger and reach $20 \cdot 10^{-4} \text{ \AA}^2$. This is indicative of intramolecular libration vibrations of the ligands in the crystal. As expected, the libration motion of the CpMCh and CpMCot molecules is anisotropic, the maximum amplitude of librations of the molecules as a whole being observed about the L_1 axis, which virtually coincides with the metal—center-of-the-ring axis (Table 4).

In all cases, the description of molecules **2**–**5** as a "segmental" rigid body³⁹ gave the better agreement between the model and the experimental data ($R_u = 1.7\text{--}3.7\%$, $\langle \Delta U^2 \rangle^{1/2} = 0.0004\text{--}0.0007 \text{ \AA}^2$, $\sigma \langle U^2 \rangle^{1/2} = 0.0010 \text{ \AA}^2$) than that obtained in the approximation of the LTS rigid-body model.³² To avoid the known singularity associated with the planar structures of the cyclic ligands in the molecules, we included the metal atom in calculations within the framework of the above-mentioned model. The calculated rms libration amplitudes ($\langle \phi^2 \rangle$) for the Cp, Ch, and Cot ligands in the crystals of **2**–**5** are also given in Table 4.

It is known that the barriers to rotation of rigid groups in crystals can be estimated based on anisotropic atomic displacements determined from X-ray or neutron diffraction data.^{31,39} The corresponding heights of the fifth-, seventh-, and eighth-order barriers, which were calculated in the harmonic approximation based on the

the $\langle \phi^2 \rangle$ values for the Cp, Ch, and Cot ligands (Table 4) are close to the analogous values for the Cp ligand in vanadocene Cp_2V (8.9 kJ mol^{-1}).³² Analysis of the published data demonstrated that the highest barriers to rotation of the unsubstituted Cp ligands in metallocenes were observed only in the orthorhombic phases of ferrocene and ruthenocene ($23\text{--}38 \text{ kJ mol}^{-1}$).⁴⁰

Taking into account the libration corrections (see Table 2), the principal geometric characteristics of the ligands in complexes **1**–**5** are almost identical, the average C—C bond length in the ligands remaining virtually independent of the size of the ligand and the nature of the metal atom. The observed changes in the M—C bond lengths and in the distances from the metal atom to the centers of the rings correlate with a decrease in the ionic radii of the metal atoms in the series of metallocenes **2**–**5**. However, the changes in the Cp—M and Ch—M distances in the CpMCh complexes are different. Thus, the Ch—M distances in the pair of compounds **2** and **3** and in the pair of **3** and **4** decrease by 0.23 and 0.30 Å, respectively, whereas the analogous changes in the distances from the metal atom to the center of the Cp ligand are 0.65 and 0.87 Å, respectively. The relative decreases in the Cp—M and Ch—M distances in the series of metallocenes **2**–**5** are identical. It should be noted that the Cp—M distance remains virtually unchanged in the case of replacement of one of the Cp ligands in Cp_2V by Ch (cf., for example, complexes **1** and **3**), whereas this distance in CpTiCot is substantially larger (by 0.047 Å) compared to that in CpTiCh.

Electron density distribution. To reveal the effect of the nature of metal and the size of the ligand on the character of the metal—(π -system) interaction, we analyzed the deformation electron density (DED) maps. Since complexes **2**–**5** are isostructural, the effect of the crystal packing on the distribution $\rho(r)$ should be identical and, consequently, the differences in the deformation electron density distribution in the series of the CpMCh and CpMCot complexes should be determined primarily by the nature of the metal atom and the ligand. The DED maps were calculated based on the results of high-angle refinement of the X-ray diffraction data (reflections with $\sin\theta/\lambda > 0.65 \text{ \AA}^{-1}$ were used).

In all sections of the deformation electron density in the planes of the cyclic ligands (Fig. 4), maxima of the same type were revealed on the C—C and C—H bonds. On the whole, the DED distributions in the Cp ligands in symmetrical and mixed metallocenes are similar in character. The exception is an insignificant increase in the DED maximum on the C(3)—C(3a) bond in CpMCh ($M = \text{Ti, V, or Cr}$), which is observed irrespective of the nature of metal. Apparently, this is associated with the fact that the crystallographic plane m passes through this bond (it is known that errors in this plane are higher²⁹).

The DED maps for compounds **1**–**5** are characterized by the anisotropy of the deformation electron density distribution about the metal atoms. Since the DED

Table 4. Eigenvalues of the libration tensor L , the rms libration amplitudes of the cyclic ligands $\langle \phi^2 \rangle$, and their rotation barriers B_n in the crystal structures of complexes **2**–**5**

Struc- ture	L_1 deg ²	L_2	L_3	Ligand	$\langle \phi^2 \rangle$	B_n /kJ mol ⁻¹
2	30.6(5)	4.6(5)	3.7(5)	Cp	41.5(6)	7.8(8)
				Ch or Cot	29.4(6)	5.7(8)
3	30.6(4)	4.6(5)	3.7(5)	Cp	38.2(5)	5.6(8)
				Ch or Cot	19.9(5)	5.6(8)
4	49.0(6)	6.0(6)	5.5(6)	Cp	63.0(5)	5.2(8)
				Ch or Cot	46.9(5)	3.6(8)
5	37.4(5)	7.6(4)	6.8(4)	Cp	62.8(4)	7.0(8)
				Ch or Cot	34.9(4)	5.0(8)

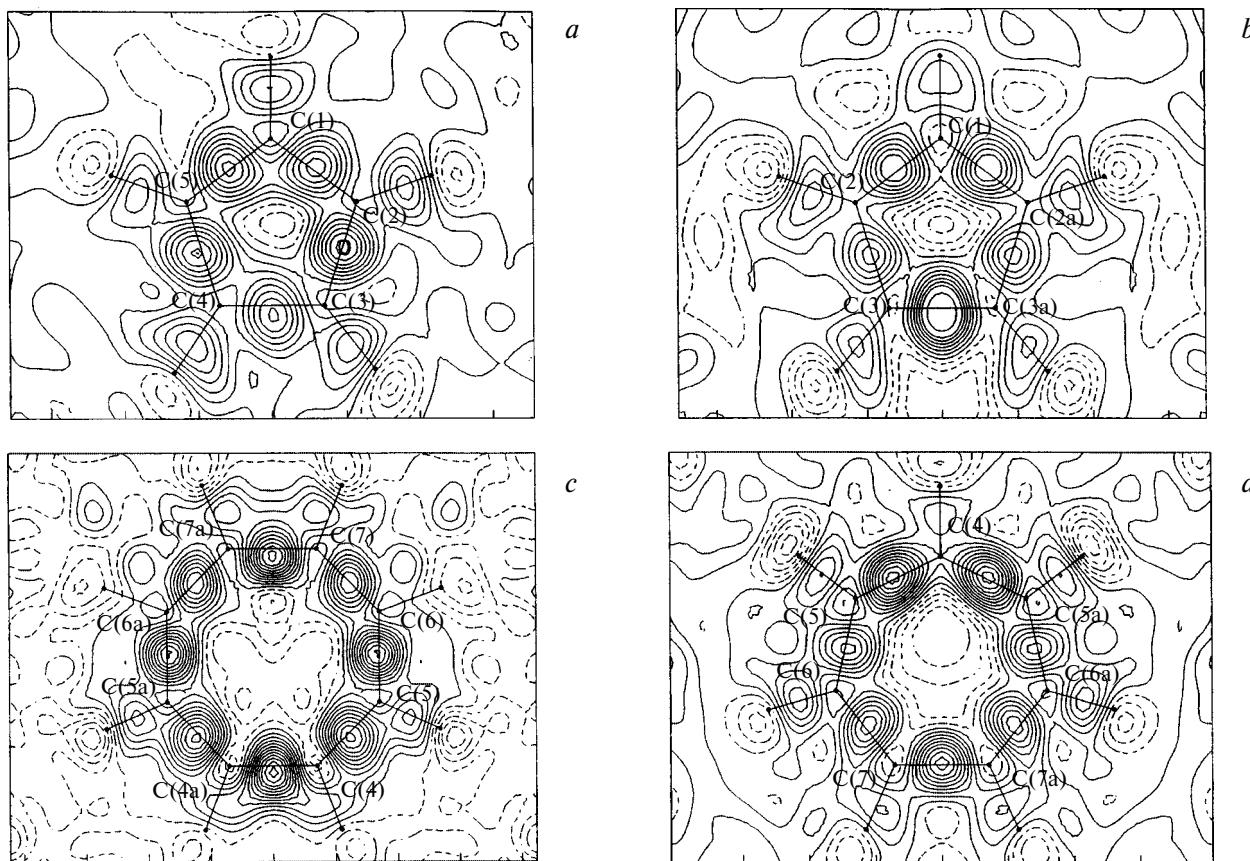


Fig. 4. Sections of the deformation electron density in the planes of the cyclic ligands of complexes **1–5**: *a*, Cp in Cp_2V ; *b*, Cp in CpVCh ; *c*, Cot in CpTiCot ; *d*, Ch in CpVCh . The zero and positives contours are shown as solid lines, and the negative contours are shown as dashed lines. Hereinafter, the maps are contoured at intervals of $0.05 \text{ e} \cdot \text{\AA}^{-3}$.

maxima in the vicinity of the metal atoms correspond to partial or complete localization of orbitals on the metal atoms, analysis of their positions and relative heights allows one to obtain qualitative and sometimes semi-quantitative estimations of the contribution of the d orbitals to the corresponding molecular orbitals of the complex.

In studies of the DED distributions, particular attention was given to analysis of the maps in the planes corresponding to the possible localization of a_1 , e_2 , and e_1 MOs. Thus, the DED sections passing through the metal atom parallel to the planes of the cyclic ligands (sections of type **A**) were constructed to analyze the population of the e_2 orbital, and the sections passing through the metal atom perpendicular to the planes of the cyclic ligands (sections of type **B**) were constructed to analyze a_1 and e_1 MOs. In addition, the sections in the crystallographic plane *m* (sections of type **C**) were analyzed for all mixed metallocenes.

Let us consider the character of the DED distribution in vanadocene. According to the published data,^{5,41} the metal atom in the ground state of vanadocene is characterized by the high-spin state ${}^4\text{A}_{2g}$ ($a_1^1 e_2^2$) and, consequently, the complex possesses three unpaired electrons. In section **A** corresponding to localization of the

e_2 orbitals of the metal atom, the virtually continuous "circular" distribution of the positive deformation electron density is observed. This distribution is similar to that in the section of the Cp ring (Fig. 5, *a*). On the whole, the distribution of the e_2 electrons can be approximately described within the framework of the cylindrical symmetry, which corresponds to the traditional description of the chemical bonds in metallocenes in the MO approximation.

The section of type **B** (see Fig. 5, *b*) in the structure of vanadocene has DED maxima with the height of $0.25 \text{ e} \cdot \text{\AA}^{-3}$ directed from the metal atom to the centers of the rings (a_1 orbital) and maxima with the height of $0.20 \text{ e} \cdot \text{\AA}^{-3}$ in the plane parallel to the Cp ligands (e_2 orbital). The presence of the DED maximum corresponding to the region of localization of the a_1 orbital indicates that the metal atom in Cp_2V is in the high-spin state. The noticeable ellipticity of the DED maximum at the midpoint of the $\text{C}(2)-\text{C}(3)$ bond in this section is also indicative of electron delocalization in the Cp ligand.

In the section of type **B** in the Cp_2V complex, the regions of depletion or the DED minima ($-0.25 \text{ e} \cdot \text{\AA}^{-3}$) in the vicinity of the metal atom along the $\text{C}(5a)-\text{V}-\text{C}(5)$ direction correspond to the e_1 orbitals, *i.e.*, the electron density transfer from the Cp ligand to

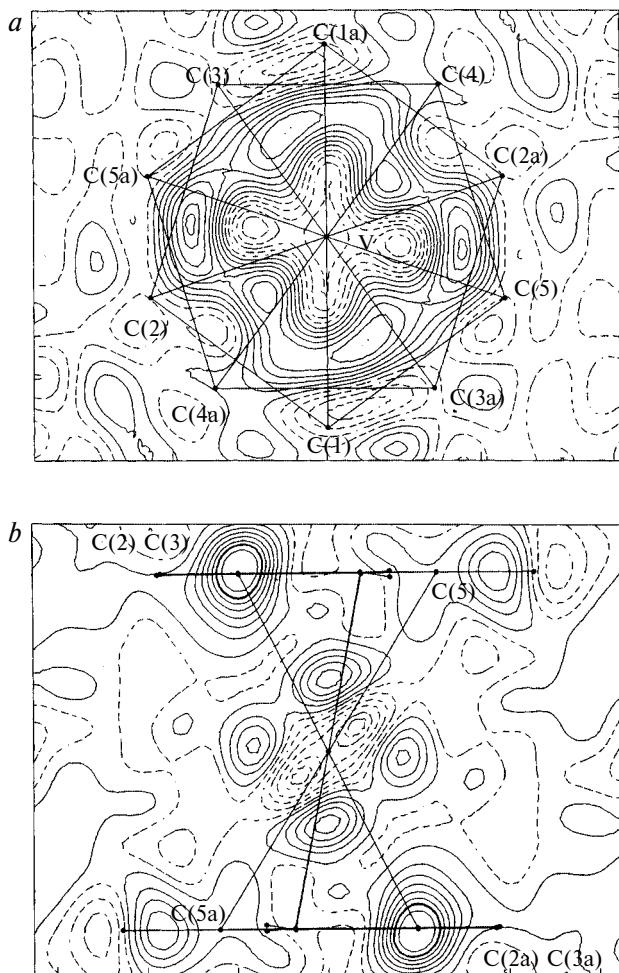


Fig. 5. Sections of the deformation electron density of the Cp_2V complex: *a*, the section of type **A** passing through the vanadium atom parallel to the plane of the Cp ligands; *b*, the section of type **B** passing through the V , $\text{C}(5)$, and $\text{C}(5\text{a})$ atoms and the midpoints of the $\text{C}(2)$ – $\text{C}(3)$ and $\text{C}(2\text{a})$ – $\text{C}(3\text{a})$ bonds.

the metal atom is either absent or very small in contrast to the results of quantum-chemical calculations.⁴ The character of the DED distribution in other sections of type **B** in vanadocene is similar to that described above.

On going from symmetrical vanadocene to mixed complexes **2–5**, the character of the DED distribution about the metal atom changes substantially. According to the theoretical concepts, the configuration of the metal atom in the CpMCh complexes changes from e_2^4 in 16-electron CpTiCh to a_1^2e_2^4 in 18-electron CpCrCh . In this connection, the DED maxima in the vicinity of the metal atom in the CpTiCh compound should be observed only in the plane parallel to the ligands, whereas the character of the DED distribution for the chromium and vanadium CpMCh complexes should be similar to that observed in vanadocene.

Analysis of the deformation electron density in the sections of type **A** in the series of metallocenes CpMCh (Fig. 6) demonstrated that the electron density in all

complexes is accumulated in the region of localization of the e_2 orbitals, which indicates that the formal charge -3

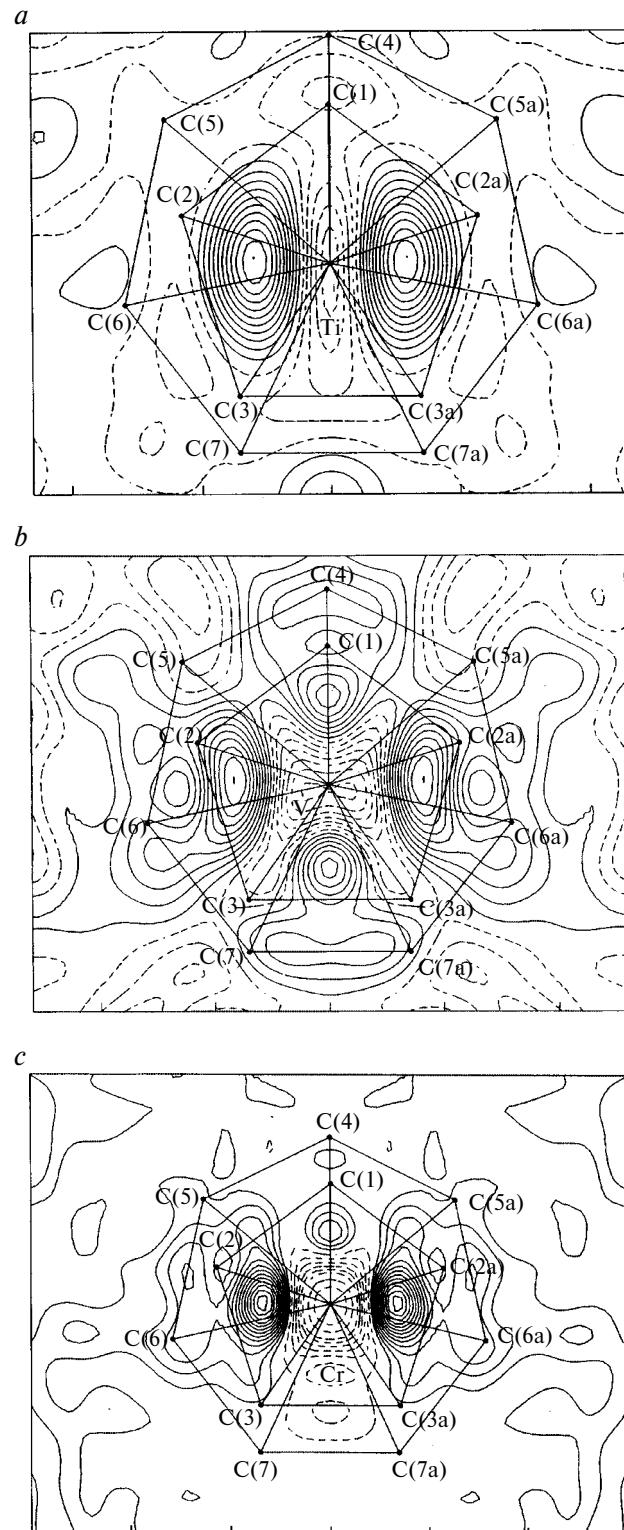


Fig. 6. Sections of the deformation electron density of type **A** in mixed metallocenes CpMCh (**2–4**): *a*, CpTiCh ; *b*, CpVCh ; *c*, CpCrCh .

assigned to the Ch ligand is inconsistent with the real electron density distribution in this type of compounds.

Yet another essential difference in the DED distribution in the sections of type **A** in the CpMCh complexes compared to that of vanadocene is the lower symmetry of the DED maxima. In this case, the character of accumulation of the deformation electron density corresponding to the e_2 orbitals in the series of CpMCh (see Fig. 6) depends on the nature of metal, although, according to theoretical considerations, the population of this doubly degenerate MO in the series of metallocenes under study should be constant in spite of the possible difference in the degree of the $e_2(\text{metal}) \rightarrow e_2(\text{Ch})$ charge transfer. Thus, the section of type **A** in the CpTiCh complex has two pronounced DED maxima ($0.52 \text{ e} \cdot \text{\AA}^{-3}$) located between the C(2) and C(2a) atoms of the Cp ligand and between the midpoints of the C(5)–C(6) and C(5a)–C(6a) bonds of the Ch ligand. In addition to two maxima ($0.44 \text{ e} \cdot \text{\AA}^{-3}$) similar to those mentioned above, two DED maxima with the height of $0.25 \text{ e} \cdot \text{\AA}^{-3}$ are located on the symmetry plane in the analogous vanadium complex. Two significant maxima ($0.65 \text{ e} \cdot \text{\AA}^{-3}$) on the symmetry plane and one additional small peak ($0.15 \text{ e} \cdot \text{\AA}^{-3}$) between the C(1) and C(4) atoms are observed in the chromium complex. Therefore, the symmetry of the distribution of the e_2 electrons in all complexes under consideration is not higher than the local symmetry C_s of the complexes. Although the DED peaks in the vicinity of the metal atom are localized only between some carbon atoms of the ligands, no substantial changes in the C–C and M–C bond lengths are observed in this series of compounds. Apparently, this fact speaks in favor of the statement that the geometry of the molecules (in particular, the bond lengths) is a rather "conservative" characteristic of the electron density distribution.

The populations of the a_1 orbitals in the vanadium and chromium (but not in titanium) complexes are manifested in the sections of type **B** (Fig. 7). As in the case of the Cp_2V complex, the deformation electron density in these sections is accumulated symmetrically with respect to the metal atom in the direction toward the centers of the ligands (a_1 orbital) and in the plane parallel to the ligands (e_2 orbitals). The regions of depletion of the electron density, which apparently correspond to the e_1 orbitals, are located along the M–C(2) and M–C(6) diagonals and the lines between M and the midpoints of the C(5)–C(6) and C(2a)–C(3a) bonds. To the contrary, the section of type **B** in metallocene CpTiCh has regions of DED depletion ($-0.25 \text{ e} \cdot \text{\AA}^{-3}$) located along the metal–center-of-the-ring direction. This is in agreement with the data of photoelectron spectroscopy and quantum-chemical calculations.⁴ The character of the DED maxima at the midpoints of the C(2)–C(3) and C(2)–H(2) bonds of the Cp ligand differs from that observed in Cp_2V . Thus the maxima in CpVCh and CpCrCh are polarized toward the 3d orbitals of the metal atoms, whereas the DED maximum in

CpTiCh is polarized in the vicinity of the titanium atom toward the midpoint of the C(5)–C(6) bond of the Ch ligand. Therefore, no accumulation of the electron den-

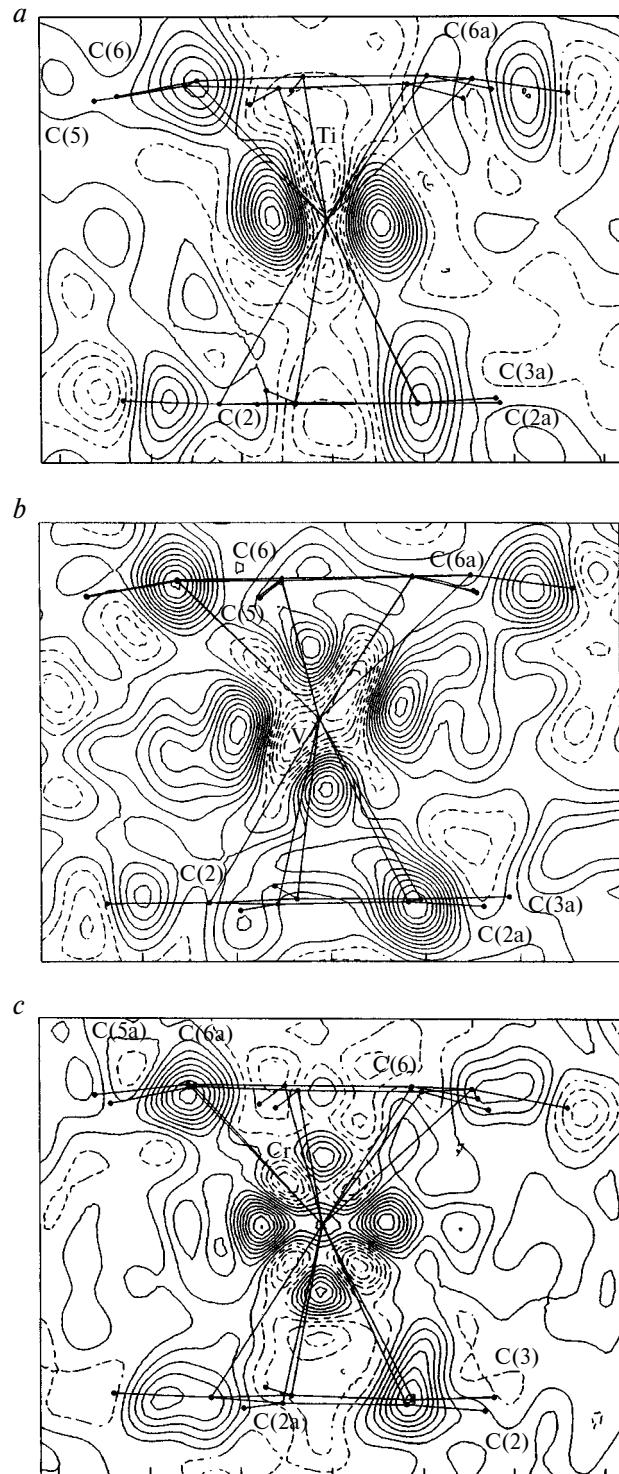


Fig. 7. Sections of the deformation electron density of type **B** passing through the C(2) and C(6a) atoms and the midpoints of the C(5)–C(6) and C(2a)–C(3a) bonds in mixed metallocenes CpMCh: *a*, CpTiCh; *b*, CpVCh; *c*, CpCrCh.

sity is observed in sections of type **B** in symmetrical and mixed metallocenes CpMCh in the region corresponding to the positions of the e_1 orbitals of the metal atom.

On going to sections of type **C** passing through the symmetry planes of the molecules (Fig. 8), the character of the electron density distribution changes. Thus, the DED maxima with approximately equal heights ($0.35 \text{ e} \cdot \text{\AA}^{-3}$ and $0.50 \text{ e} \cdot \text{\AA}^{-3}$) are localized in this plane along the diagonal C(4)—M—the midpoint of the C(3)—C(3a) bond in the CpTiCh and CpVCh compounds, respectively. The sections of types **B** and **C** in the chromium complex are also different in spite of the absence of accumulation of the deformation electron density in the diagonal direction. As can be seen from Fig. 6, only one weak DED maximum is observed in the vicinity of the metal atom on the side of the C(1) and C(4) atoms in the plane parallel to the cyclic ligands of the CpCrCh compound. Although the DED peaks in sections of type **C** correspond to localization of the e_1 orbital, it is highly improbable that these peaks are attributed to the e_1 antibonding orbitals taking into account the peak heights and the absence of the symmetrical DED maximum along the diagonal C(1)—M—the midpoint of the C(7)—C(7a) bonds.

As is evident from lowering of the symmetry of the peak arrangement in the sections of type **A** and the presence of additional DED maxima in the sections of type **C**, the chemical bonds in mixed metallocenes, unlike those in symmetrical metallocenes, cannot be adequately analyzed in the approximation of the cylindrical symmetry. This suggestion is supported by the above-mentioned symmetry C_s of the molecules in the crystal and the substantial deviation of the H(1) atom from the plane of the Cp ligand in addition to the character of the DED distribution. This result casts doubt on the correctness of the use of the approximation of the cylindrical symmetry in analysis of the contribution of the 3d orbitals to the molecular orbitals of the CpMCh complexes for interpreting photoelectron spectra.

Mixing of the a_1 , e_2 , and e_1 molecular orbitals is one of the possible reasons for the appearance of additional DED maxima in the symmetry plane of metallocenes CpMCh. It should be noted that (according to the data of quantum-chemical calculations⁴ and physicochemical studies^{9,11,15}) splitting between the a_1 and e_2 levels is always smaller than that between the e_1 and a_1 levels. According to the data of photoelectron spectroscopy, this splitting decreases from 1.6 to 0.25 eV on going from CpCrCh to CpTiCh (for comparison, splitting between a_1 and e_2 MOs in CpTiCot is 1.95 eV). Consequently, mixing of a_1 and e_2 MOs is most probably responsible for the appearance of additional DED maxima (along with the expected maxima) in the CpTiCh and CpCrCh complexes.

The CpTiCot complex is formally isoelectronic ($e_2^2 a_1^1$) to the CpVCh complex. However, according to the results of calculations by the INDO method, the contribution of the metal atom to e_2 MO of metallocene

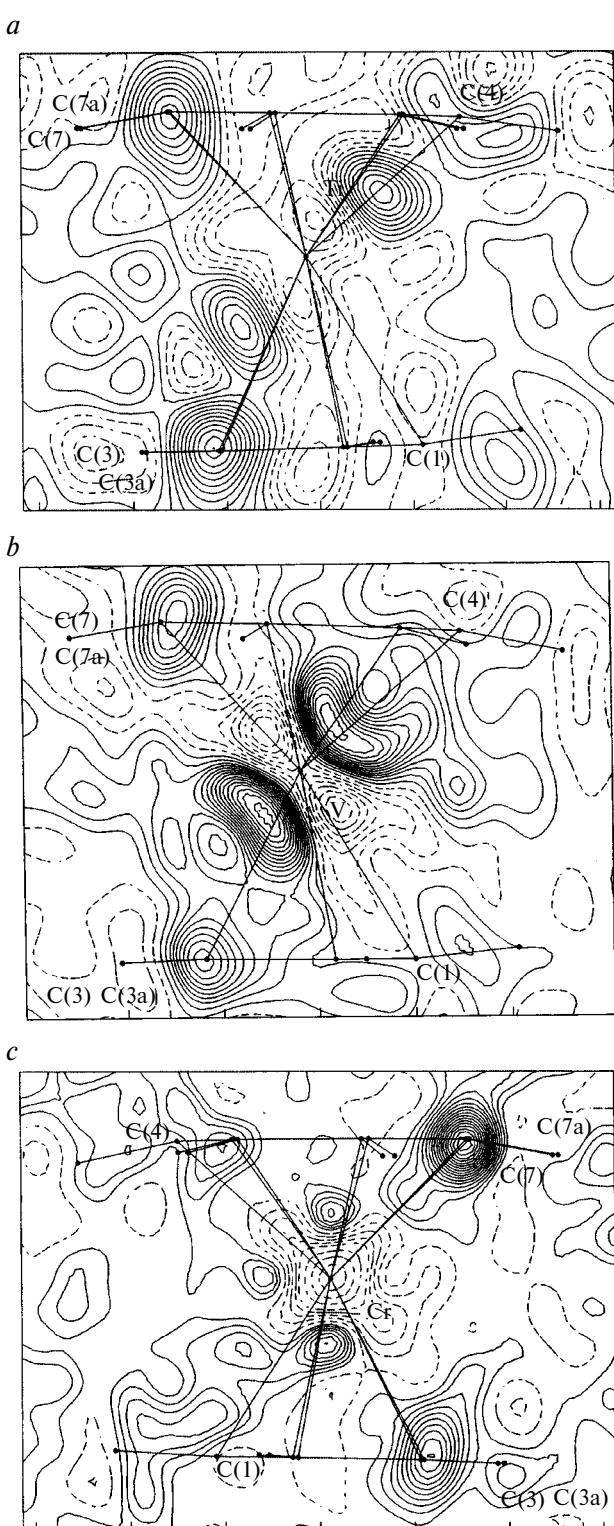


Fig. 8. Sections of the deformation electron density of type **C** passing through the symmetry plane m in mixed metallocenes CpMCh: *a*, CpTiCh; *b*, CpVCh; *c*, CpCrCh.

is no higher than 20%¹³ due to a substantial decrease in the energy of the e_2 orbitals of the Cot ligand. To the

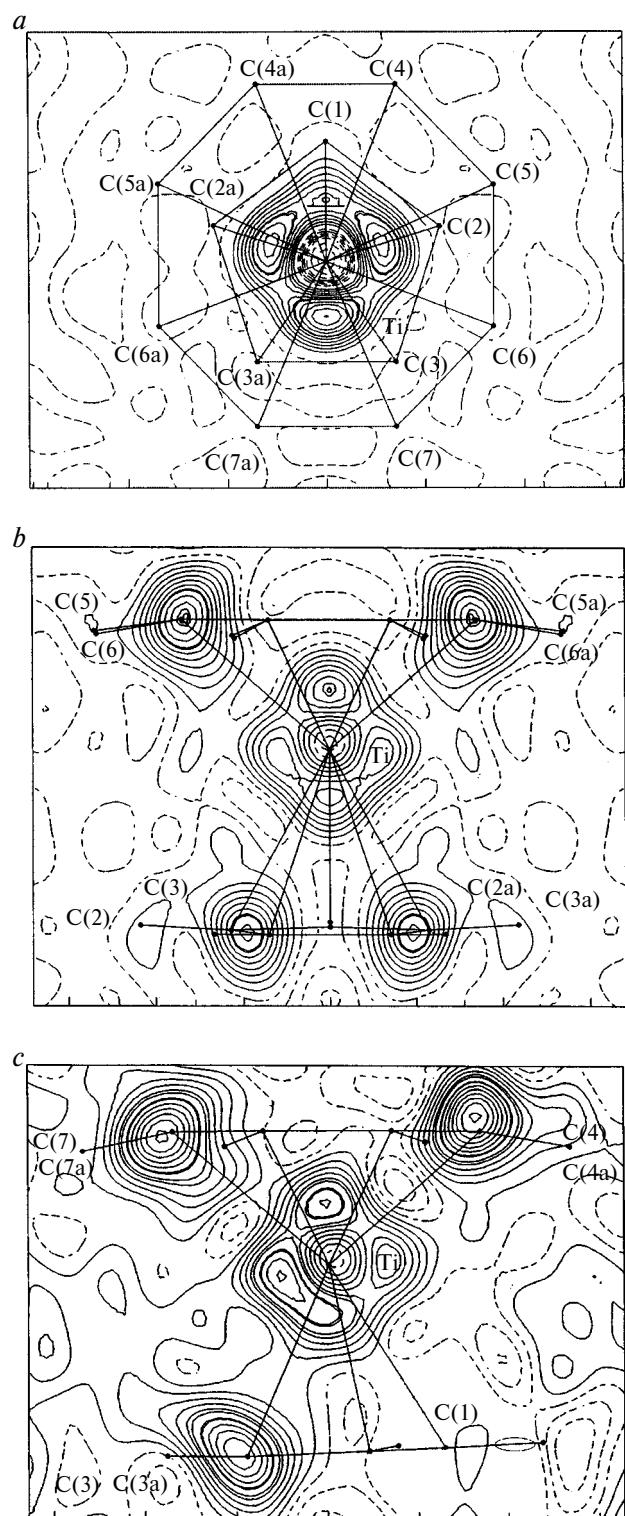


Fig. 9. Sections of the deformation electron density of the CpTiCot complex: *a*, the section of type **A** passing through the titanium atom parallel to the plane of the Cp and Cot ligands; *b*, the section of type **B** passing through the Ti atom and the midpoints of the C(2)—C(3), C(2a)—C(3a), C(5)—C(6), and C(5a)—C(6a) bonds; *c*, the section of type **C** passing through the symmetry plane *m*.

contrary, the section of type **A** shows substantial accumulation of the deformation electron density in the plane corresponding to localization of e_2 MO (Fig. 9). The DED maxima corresponding to the positions of the e_2 orbitals of the metal atom are continuous "circular" in character like those observed in vanadocene (see Fig. 5). Consequently, the DED maps and the data of photo-electron spectroscopy⁹ (see Table 1) are indicative of a substantial contribution of the 3d orbitals of the metal atom to the e_2 orbitals of the CpMCh and CpMCot complexes.

An interesting feature of the DED distribution in the section of type **B** in the CpTiCot complex is the asymmetry of the maxima directed from the metal atom to the centers of the rings. As can be seen from Fig. 9, the DED maximum directed toward the Cot ligand in the section passing through the metal atom and the midpoints of the C(5)—C(6), C(2)—C(3), C(5a)—C(6a), and C(2a)—C(3a) bonds is higher (0.40 $e \cdot \text{\AA}^{-3}$) than that directed toward the Cp ligand (0.30 $e \cdot \text{\AA}^{-3}$). Taking into account the decrease in the distance from the metal atom to the center of the Cot ligand (1.441 Å) compared to the analogous distance in CpTiCh (1.487 Å), it can be assumed that the observed asymmetry of the DED distribution in section **B** occurs due to partial overlapping of the a_1 orbital with the π -system of the Cot ligand. The major difference between the CpTiCot compound and the mixed CpMCh complexes is the absence of accumulation of the deformation electron density along the diagonal directions in section **C**. Apparently, the character of the metal—(π -ligand) chemical bond in CpTiCot is more similar to that observed in vanadocene than to that observed in the mixed CpMCh complexes.

Investigation of the electron density distribution in symmetrical and mixed metallocenes demonstrated that the character of the M—(π -ligand) chemical bond depends substantially on the nature of the metal atom and the size of the cyclic ligand in spite of the similarity of the geometric parameters of the ligands. Accumulation of the deformation electron density in mixed metallocenes in sections corresponding to the e_2 orbitals of the metal atom indicates that the formal charge -3 of the cycloheptatrienyl ligand does not correspond to the real electron density distribution in the CpMCh complex. In turn, accumulation of the deformation electron density in the analogous section in CpTiCot indicates that the contribution of the ligand to the e_2 MO of the complex calculated by the quantum-chemical method (INDO) is overestimated. This casts doubt on the change in the order of molecular orbitals obtained in calculations by the INDO method.⁴

Comparison of the DED maps of vanadocene and mixed metallocenes demonstrated that lowering of the local symmetry of the complexes to C_s leads to a substantial change in the electron density distribution. This casts doubt on the correctness of the description of the chemical bond in mixed metallocenes CpMCh in the approximation of the cylindrical symmetry. To the con-

trary, the character of the DED distribution in CpTiCot is similar to that observed in vanadocene.

Experimental

The detailed results of investigation of the electron density distribution in vanadocene and the nature of disorder of the Cp ligands in the crystals have been published previously.^{25,32}

Well-faceted single crystals of compounds **2–5** were prepared by slow sublimation *in vacuo*. X-ray diffraction data sets were collected from samples of linear dimensions of ~0.3 mm on a four-circle Siemens P3/PC diffractometer (graphite monochromator, Mo-K α radiation, $\theta/2\theta$ scanning technique). In the region of small diffraction angles ($\sin\theta/\lambda < 0.65 \text{ \AA}^{-1}$), reflections were measured within the total sphere of the reciprocal space. High-angle reflections were measured within at least two independent octants. Empirical absorption corrections were applied using the azimuth scanning technique.

The structures were solved by direct methods and refined anisotropically by the full-matrix least-squares method. The positions of the hydrogen atoms were revealed from difference electron density syntheses and included in the final refinement with isotropic thermal parameters. The precise positional and thermal parameters of the nonhydrogen atoms were determined by the high-angle refinement (reflections with $\sin\theta/\lambda > 0.65 \text{ \AA}^{-1}$ were used). All calculations were carried out with the use of the SHELXTL PLUS program package (see Table 1).

We thank J. C. Green (Inorganic Chemistry Laboratory, Oxford University) for supplying samples of $(\eta^5\text{-C}_5\text{H}_5)\text{V}(\eta^5\text{-C}_7\text{H}_7)$.

This work was financially supported by the Russian Foundation for Basic Research (Project Nos. 00-15-97359, 00-03-32807a, 99-07-90133, 00-03-32853, and 00-15-97439).

References

- J. P. Collman, L. S. Hegedaus, J. R. Norton, and R. G. Finke, *Principles and Applications of Organotransition Metal Chemistry*, University Science Books, Mill Valley, 1987.
- P. Laszlo and R. Hoffmann, *Angew. Chem., Int. Ed.*, 2000, **39**, 123.
- M. A. Beswick, J. S. Palmer, and D. S. Wright, *Chem. Soc. Rev.*, 1998, **27**, 225.
- D. W. Clack and K. D. Warren, *Structure and Bonding*, 1980, **39**, 1.
- M. L. H. Green and D. K. P. Ng, *Chem. Rev.*, 1995, **95**, 439.
- E. M. Shustorovich and M. E. Dyatkina, *Dokl. Akad. Nauk SSSR*, 1959, **128**, 1729 [*Dokl. Chem.*, 1959 (Engl. Transl.)].
- G. Cooper, J. C. Green, and M. P. Payne, *Mol. Phys.*, 1988, **63**, 1031.
- F. G. N. Cloke, A. Dix, J. C. Green, R. N. Perutz, and E. A. Seddon, *Organometallics*, 1983, **2**, 1150.
- C. E. Davies, I. M. Gradiner, J. C. Green, M. L. H. Green, N. J. Hazel, P. D. Grebenik, V. S. B. Mtetwa, and K. Prout, *J. Chem. Soc., Dalton Trans.*, 1985, 669.
- J. C. Green, M. L. H. Green, N. Kaltsoyannis, P. Mountford, P. Scott, and S. J. Simpson, *Organometallics*, 1992, **11**, 3353.
- J. C. Green, N. Kaltsoyannis, Kong Hung Sze, and M. MacDonald, *J. Am. Chem. Soc.*, 1994, **116**, 1994.
- R. D. Fisher, *Theor. Chim. Acta*, 1963, **1**, 418.
- D. W. Clack and K. D. Warren, *Inorg. Chim. Acta*, 1977, **24**, 35.
- D. W. Clack and K. D. Warren, *Theor. Chim. Acta*, 1977, **46**, 313.
- S. Evans, J. C. Green, S. E. Jackso, and B. Higginson, *J. Chem. Soc., Dalton Trans.*, 1974, 304.
- R. R. Andrea, A. Terpstra, and A. Oskam, *J. Organomet. Chem.*, 1986, **81**, 307.
- D. Gourier and E. Samuel, *Inorg. Chem.*, 1988, **27**, 3018.
- C. J. Groenenboom, H. J. De Liefde Meijer, and F. Jellinek, *J. Organomet. Chem.*, 1974, **69**, 235.
- C. J. Groenenboom, G. Sawatzky, H. J. De Liefde Meijer, and F. Jellinek, *J. Organomet. Chem.*, 1974, **76**, C4.
- C. J. Groenenboom, G. Sawatzky, H. J. De Liefde Meijer, and F. Jellinek, *J. Organomet. Chem.*, 1975, **97**, 73.
- M. Vliek, C. J. Groenenboom, H. J. De Liefde Meijer, and F. Jellinek, *J. Organomet. Chem.*, 1975, **97**, 67.
- R. Weits, B. Rees, A. Mitshlier, and F. Mathey, *Inorg. Chem.*, 1981, **20**, 2966.
- R. Goddard and C. Kruger, in: *Electron Distributions and the Chemical Bond*, Ed. P. Cappens, McGraw Hill, New York, 1982, 297.
- M. Yu. Antipin, K. A. Lyssenko, and R. Boese, *J. Organomet. Chem.*, 1996, **508**, 259.
- Y. Wang, K. Angermund, R. Goddard, and C. Kruger, *J. Am. Chem. Soc.*, 1987, **109**, 587.
- A. Mitschler, B. Rees, and M. S. Lehmann, *J. Am. Chem. Soc.*, 1978, **100**, 3390.
- Y. Wang and P. Cappens, *Inorg. Chem.*, 1975, **15**, 1122.
- P. Cappens, *Coord. Chem. Rev.*, 1985, **65**, 285.
- M. Yu. Antipin and Yu. T. Struchkov, *Metalloorg. Khim.*, 1989, **2**, 128 [*Organomet. Chem. USSR*, 1989, **2** (Engl. Transl.)].
- A. A. Low and M. B. Hall, in: *Theoretical Models of Chemical Binding, Part 2, The Concept of the Chemical Bond*, Ed. Z. B. Maksiz, Springer-Verlag, Berlin, 1990, 543.
- M. Yu. Antipin and R. Boese, *Acta Crystallogr.*, 1996, **B52**, 314.
- V. Schomaker and K. N. Trueblood, *Acta Crystallogr.*, 1968, **B24**, 63.
- F. L. Hirshfeld, *Acta Crystallogr.*, 1976, **A32**, 239.
- J. D. Zeinstra and J. L. de Boer, *J. Organomet. Chem.*, 1973, **54**, 207.
- R. E. Rundle and G. Engebreton, *J. Am. Chem. Soc.*, 1963, **85**, 481.
- P. A. Kroon and R. B. Helmholtz, *J. Organomet. Chem.*, 1971, **31**, 71.
- G. A. Olah, G. K. S. Prakash, R. E. Williams, L. D. Filed, and K. Wade, *Hypercarbon Chemistry*, J. Wiley and Sons, New York, 1987.
- T. Maverick and K. N. Trueblood, *Thermal Motion Analysis Program THMA-11*, Zürich, 1987.
- T. Maverick and J. D. Dunitz, *Mol. Phys.*, 1987, **62**, 451.
- P. Seiler and J. D. Dunitz, *Acta Crystallogr.*, 1980, **B36**, 2255.
- A. Haaland, *Acc. Chem. Res.*, 1979, **12**, 415.

Received April 25, 2000;
in revised form September 14, 2000